Precision atom interferometry

A. Peters, K. Y. Chung, B. Young, J. Hensley and S. Chu

Email alerting service	Receive free email alerts when new articles cite this article - sign up in the box at the top right-hand corner of the article or click **here**

Precision atom interferometry

By A. Peters, K. Y. Chung, B. Young, J. Hensley and S. Chu

Physics Department, Stanford University, Stanford, CA 94305, USA

The basic physical principles behind atom interferometers based on optical pulses of light are summarized. This method of atom interferometry is based on measurements in the time and frequency domain and is an inherently precise measurement technique. After a brief discussion of some of the important technical requirements for good fringe accuracy and visibility, we describe an interferometer that has measured the acceleration of an atom due to gravity with a resolution better than one part in 10^{10}. We project that the absolute accuracy of our measurement will be of the order of a few parts in 10^9. We also describe an interferometer experiment that measures the recoil energy shift of an atom when it absorbs a photon. When combined with the value of the Rydberg constant and the mass ratios $M_{\mathrm{Cs}}/m_{\mathrm{p}}$ and $m_{\mathrm{p}}/m_{\mathrm{e}}$, one can obtain a value for α, the fine structure constant. Currently, we have an experimental resolution $\Delta\alpha/\alpha \sim 10^{-8}$ after two hours of integration time and are studying the systematic effects that affect the measurement.

1. Introduction

The first realizations of atom interferometers in 1991 marked the introduction of a new measuring device. Following this work, a number of novel interferometers and atom optics components that could be used in atom interferometers have been proposed or demonstrated (see, for example, Berman 1997). Our work in this area was guided by the desire to exploit a number of inherent advantages of atom interferometers. (i) Laser cooling and manipulation techniques extend the interferometer measurement time, defined as the drift time of an atom through the interferometer, by orders of magnitude over interferometers based on photons, electrons or neutrons. (ii) The effects of beamsplitters and mirrors based on optical pulses can be calculated to high precision since the interactions of light with matter are well understood. (iii) The internal degrees of freedom of an atom offer the possibility of designing better interferometer components.

This article gives a physically intuitive derivation of the interferometer phase shift and summarizes the current status of two atom interferometers based on counterpropagating optical light pulses developed at Stanford. Although most of the discussion will focus on the interferometer used to measure g, the acceleration due to gravity, much of the analysis carries over to the measurement of $\hbar/M_{\mathrm{Cs}}$. Earlier versions of this work have been described in Kasevich & Chu (1991, 1992), Weiss *et al.* (1993, 1994), Weitz *et al.* (1994*a*,*b*) and Young (1997).

2. Calculation of the interferometer phase shift

Consider a series of optical pulses used to construct an atom interferometer which measures the acceleration of gravity. The pulses cause the atom to enter a superposition of different internal states that spatially separate and recombine. From Feynman's formulation of quantum mechanics (Feynman & Hibbs 1965), the wave function $\Psi(z_b, t_b)$ at a spacetime point (z_b, t_b) is due to the contributions from all points (z_a, t_a), (z'_a, t'_a), (z''_a, t''_a), ... that end up at point (z_b, t_b). For the contribution due to point (z_a, t_a), the wave function is given by $\Psi(z_b, t_b) = e^{iS_{\mathrm{Cl}}/\hbar}\Psi(z_a, t_a)$, where the classical action S_{Cl} is given by

$$S_{\mathrm{Cl}} = \int_{t_a}^{t_b} L(z, \dot{z})\,\mathrm{d}t, \quad L(z, \dot{z}) = \tfrac{1}{2}M\dot{z}^2 - Mgz. \tag{2.1}$$

This expression is valid if the classical action S_{Cl}, defined by the integral over a path where the action is an extremum, is much greater than $\hbar$. Otherwise, we must sum the contributions to the action due to all allowed paths connecting (z_a, t_a) with (z_b, t_b).

Since the phase shift is evaluated along the classical paths, the calculation is particularly simple. Consider an atom initially in internal state $|1\rangle$ with some spatial and initial momentum distribution. (If the atoms are prepared in optical molasses, each atom will be localized to roughly $\Delta x \sim \lambda$, where λ is the wavelength of light, and have a momentum spread of at least $\Delta p \sim \hbar/\lambda$.) We decompose the atomic state into a superposition of momentum plane wave states. At the point (z_a, t_a), the part of the atom in the state $|1, p\rangle$ is exposed to a $\tfrac{1}{2}\pi$ pulse, causing this atomic state to enter into a superposition of the states $|1, p\rangle$ and $|2, p+\hbar k\rangle$, where the contribution $\hbar k$ is the momentum recoil due to the absorption of a photon. The atom is then allowed to drift in the dark, until a time T when a π pulse is applied. This pulse causes the part of the atom in the state $|1, p\rangle$ to make a transition into state $|2, p+\hbar k\rangle$ and the part of the atom in state $|2, p+\hbar k\rangle$ to make a transition to the state $|1, p\rangle$. Finally, at time $2T$, the two parts of the wave function spatially overlap, and a second $\tfrac{1}{2}\pi$ is applied to the atom. The final wave function $\Psi(z_b, t_b)$ at spacetime point (z_b, t_b) is composed of contributions from the different momentum components p, p', p'', ..., originating at different points (z_a, t_a), (z'_a, t'_a), (z''_a, t''_a), ..., such that the final end point (z_b, t_b) is the same.

We will show that each momentum component of the atom will experience the same net phase shift. (In this approximation, we ignore phase shifts due to the gravitational gradient.) Thus, the interferometer contrast is not degraded by the momentum distribution of each atom or by the spread in the momenta of the ensemble of atoms as long as the optical pulses are $\tfrac{1}{2}\pi$ and π pulses for all atoms in the ensemble. If the pulses are sufficiently short, the frequency spectrum $\delta\nu \sim 1/\tau$, where τ is the pulse width, will be broad enough to generate approximately equal area pulses for all of atoms in the velocity distribution. In the limit where the Doppler width due to the velocity distribution is much broader than $\delta\nu$, the maximum fringe contrast is 28% (Kasevich & Chu 1992). Because the phase shifts are the same for all momenta and because the interferometer signal is read out in terms of a population difference between internal states, well collimated atomic beams that sacrifice flux are not needed.

The phase shift can be decomposed into two parts: the evolution of the atom during the time the light is on and the free-falling evolution of the atom. One can easily show
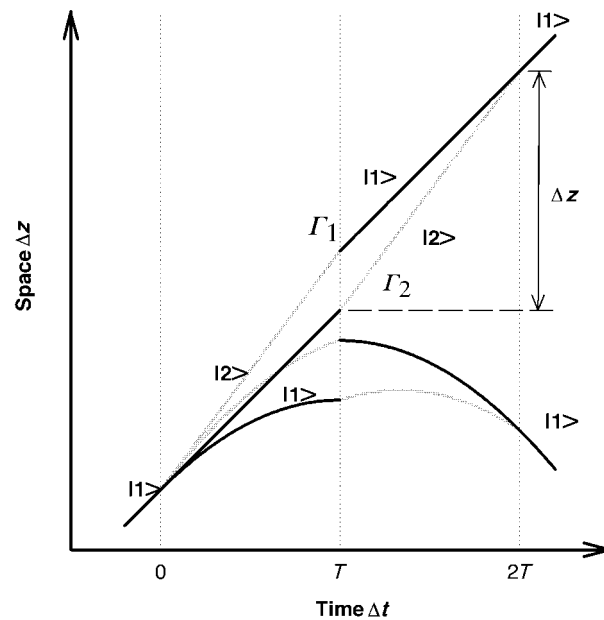
Figure 1. Phase space diagram of the atom interferometer based on the $\frac{1}{2}\pi - \pi - \frac{1}{2}\pi$ pulse sequence, showing paths in both absence and presence of gravity. The momentum pulses due to the off-resonant Raman pulses are assumed to be directed upwards. The pulse timing is chosen so that the π pulse is applied near the top of the fountain. The amplitude $|\Psi(z_b, 2T)\rangle$ of an atom described by a wavepacket at $T = 0$ is the sum of a number of amplitudes from slightly different classical paths beginning at z_a, z'_a, z''_a, ..., and $T = 0$. A single momentum (plane wave) state of the atom is shown in the figure. Apart from gradient effects, paths with different initial momenta will give the same phase shift.

that the phase shifts due to the free evolution of the atom (equation (2.1)) along the two paths shown in figure 1 are identical. Thus, the net phase shift measured by the interferometer is due to the interaction of the atom with the optical fields. During the time the light is on, the phase evolution of the atom can easily be calculated using quantum mechanics. In the limit of a short pulse, the transition amplitude of an atom going from state $|1\rangle$ to $|2\rangle$ is $A_{21}e^{-i(k_L z_1 - \omega_L t_1 - \phi_1)}$, where $A_{21} = 1/\sqrt{2}$ for a $\frac{1}{2}\pi$ pulse. Here, k_L, ω_L and ϕ_1 are the wave vector, frequency and phase of the light at the point (z_1, t_1). For transitions from state $|2\rangle$ back to state $|1\rangle$, the amplitude is $A_{12}e^{-i(k_L z_1 - \omega_L t_1 - \phi_1)}$. For transitions $|1\rangle \rightarrow |1\rangle$ and $|2\rangle \rightarrow |2\rangle$, the wave function is multiplied by amplitudes A_{11} and A_{22}.

Applying the quantum mechanical rules given above, the total number of atoms in the $|1\rangle$ state after the end of the second $\frac{1}{2}\pi$ pulse is given by $|A|^2 = |A_{\Gamma_1} + A_{\Gamma_2}|^2$, where

$$A_{\Gamma_1} = \frac{1}{\sqrt{2}}\exp(-i(k_L z_1 - \omega_L t_1 - \phi_1))\frac{1}{\sqrt{2}}\exp(i(k_L z_{2,\Gamma_1} - \omega_L t_2 - \phi_2))$$

$$A_{\Gamma_2} = \frac{1}{\sqrt{2}}\exp(-i(k_L z_{2,\Gamma_2} - \omega_L t_2 - \phi_2))\frac{1}{\sqrt{2}}\exp(i(k_L z_3 - \omega_L t_3 - \phi_3)).$$

In the absence of a gravitational potential, $(z_1 - z_{2,\Gamma_1}) = (z_3 - z_{2,\Gamma_2}) \equiv \Delta z$ and $(t_2 - t_1) = (t_3 - t_2) \equiv T$, and the net phase difference between the two paths is $\Delta\phi = \Delta\phi_{\text{upper}} - \Delta\phi_{\text{lower}} = (\phi_1 - \phi_2) - (\phi_2 - \phi_3)$. In the presence of gravity, $(z_1 - z_{2,\Gamma_1}) = \Delta z - \frac{1}{2}gT^2$, while $(z_3 - z_{2,\Gamma_2}) = \Delta z - \frac{3}{2}gT^2$. Thus, the net phase

shift becomes (Kasevich & Chu 1991; Storey & Cohen-Tannoudji 1994)

$$\Delta\phi = k_{\mathrm{L}}gT^2 + (\phi_1 - \phi_2) - (\phi_2 - \phi_3). \tag{2.2}$$

Note that the phase shift is independent of the initial momentum.

The origin of the phase shift given by equation (2.2) is clear from the derivation. An atom at rest will see $\omega_{\mathrm{L}}T/2\pi$ oscillations of the applied field in a time T. On the other hand, if the atom moves a distance Δz in the same direction as the light during the same time T, it will see $k_{\mathrm{L}}\Delta z/2\pi$ fewer oscillations. The interferometer measurement of g compares the phase shift $k_{\mathrm{L}}\Delta z$ an atom experiences during the first part of the free-fall time with the phase shift during the second interval of time. Since this is a differential measurement of a phase change, a number of potentially troublesome effects such as the AC Stark shift generated by the optical fields are greatly suppressed.

The phase shift given by equation (2.2) is independent of the quantum scale factor $\hbar/M$. This might lead one to think of the phase shift measured by this atom interferometer as 'classical' and different from the 'quantum' measurement made by a neutron interferometer. We will now show that both the neutron and atom interferometer measurements of g result from the same basic quantum physics. However, an absolute measurement of g with an atom interferometer has the advantage that the interaction of an atom with a laser field is inherently better understood than the interaction of a neutron with a crystal.

In the neutron interferometer literature, the phase shift is usually calculated by dividing the Lagrangian into two terms $L = L_0 + L_1$, where L_1 is a small perturbation (see, for example, Greenberger & Overhauser 1979). To first order, the action can be calculated as the integral of the perturbative action $S' \equiv \int_{t_a}^{t_b} L_1 \, \mathrm{d}t$ along the *unperturbed* path determined by L_0†. Evaluation of this integral leads to a net phase shift given by $\Delta\phi = -(Mg/\hbar) \times$ (phase space area), where the interferometer phase space area is given by $\Delta z \times \Delta t$. Both the $M/\hbar$ and the phase space area are often cited as a measure of the sensitivity of the device. Although this formula explicitly contains g and $\hbar/M$, the area can be written in terms of the momentum transferred by the lattice of wave vector $k_{\mathrm{Lat}} = 2\pi/a$, where a is the interatomic spacing of the lattice plane causing the Bragg scattering. The area is $\Delta z \times \Delta t = (\hbar k_{\mathrm{Lat}}/M)T \times T$ so that $\Delta\phi = -k_{\mathrm{Lat}}gT^2$. Since the neutrons scatter from three portions of a single silicon crystal, the relative phases of the three lattice planes $(\phi_1 - \phi_2) - (\phi_2 - \phi_3) = 0$. Thus, this method of calculating the phase shift also gives equation (2.2). Alternatively, the same phase shift is obtained if the neutron experiments were analysed in terms of the free evolution along the gravitationally perturbed paths and the phase slip of the neutron due to gravity with respect to the lattice.

3. Technical issues related to fringe accuracy and visibility

The interferometer measurement is based on the phase shift measured by an atom moving in a travelling wave. Our atom interferometer experiments use laser cooled atoms in an atomic fountain with free-fall times up to 0.5 s. During this time, the states $|1\rangle$ and $|2\rangle$ must be stable against radiative decay. Also, if the frequency of the optical field is not stable during the drift time of the interferometer, the fringes will

† In this simplified treatment, we ignore the complications due to the dynamical scattering of neutrons in a crystal, the multiple interferometer paths taken by the neutrons and possible effective mass shifts.

wash out. Since the measurement time is so long, a change in the optical frequency of a few Hertz will cause the interferometer to cycle through 2π radians. Currently, lasers with this frequency stability do not exist.

Both of these requirements are satisfied if we use stimulated transitions between two (magnetic field insensitive) ground states of the atom separated by a hyperfine splitting. If the two laser beams k_1 and k_2 are counterpropagating, the phase shift seen by the atom is given by $(k_1 + k_2) \times \Delta z$, approximately twice the shift relative to a single beam. On the other hand, only the relative frequency of the two beams is critical for the measurement. It is relatively easy to phase lock two laser beams relative to each other, either by generating the second frequency with an electro-optic or acousto-optic device or by phase locking two independent lasers to a stable microwave reference. Thus, by inducing a two-photon transition with counterpropagating beams, the extraordinary requirement of subHertz optical stability is reduced to the much more modest demand of subHertz microwave stability. Our measurement of the acceleration due to gravity maps directly onto the phase change relative to a stable microwave reference with the conversion 'ruler' given by the absolute wavelength (and hence frequency) of the light used to induce the optical transitions.

For a free-fall time $2T = 0.32$ s, the atoms in our fountain will undergo a Doppler shift of *ca.* 7.4 MHz. Thus, the frequency difference of the two Raman beams must be changed to keep in resonance with the falling atoms. If the frequency difference of the two Raman beams were changed so as to keep exactly in resonance with the falling atoms, all of the atoms would be in state $|1\rangle$ after the final $\frac{1}{2}\pi$ pulse. Any slight difference in the frequency change between the frequency difference of the two optical beams and the falling atoms appears as a change in the population of the atoms in the excited state. In the actual experiment, we change the frequency in two discrete steps with a direct digital frequency synthesizer that changes its frequency in a phase continuous manner so that the relevant optical phase of the light is known. Nevertheless, the experimental control of the microwave electronics at our level of precision is not trivial. A precision $\Delta g/g \leqslant 10^{-10}$ corresponds to a phase change of 3×10^{-4} radians, and any *nonlinear* frequency dependent phase shifts due to the RF filters, amplifiers, electro-optic or acousto-optic modulators must be precisely known.

In our measurement of g, any change in the relative paths of the two laser beams due to vibrations or air currents will be seen as a spurious phase shift. With interferometers using conventional thermal atomic beams, the interferometer drift times are sufficiently short so that normal laboratory vibration isolation tables are adequate. However, the long interferometer times allowed by atomic fountains require that vibrations at frequencies well below 1 Hz be suppressed.

We have minimized the effects of these noise sources by constructing an actively stabilized vibrationally isolated platform (Hensley *et al.* 1997). In the case of the g measurement, the two laser beams are co-propagating and any vibrational noise added to the laser beams is common to both beams. The two beams enter the vacuum chamber and are retro-reflected back into the chamber with a mirror mounted on the stable platform as shown in figure 2. Since the linewidth of the optical transitions, governed by the Rabi frequency of the two-photon transition, is much less than the Doppler shift of the moving atoms, the moving atoms select the relevant frequency from each of the two beams that can drive the transition using the Doppler effect. Without active stabilization, the interferometer contrast goes to zero for times of the order of $T = 40$ ms. With the feedback circuit turned on, the interferometer contrast at 160 ms is roughly 97% of the contrast at 0.5 ms. In the $\hbar/M$ experiment, a similar
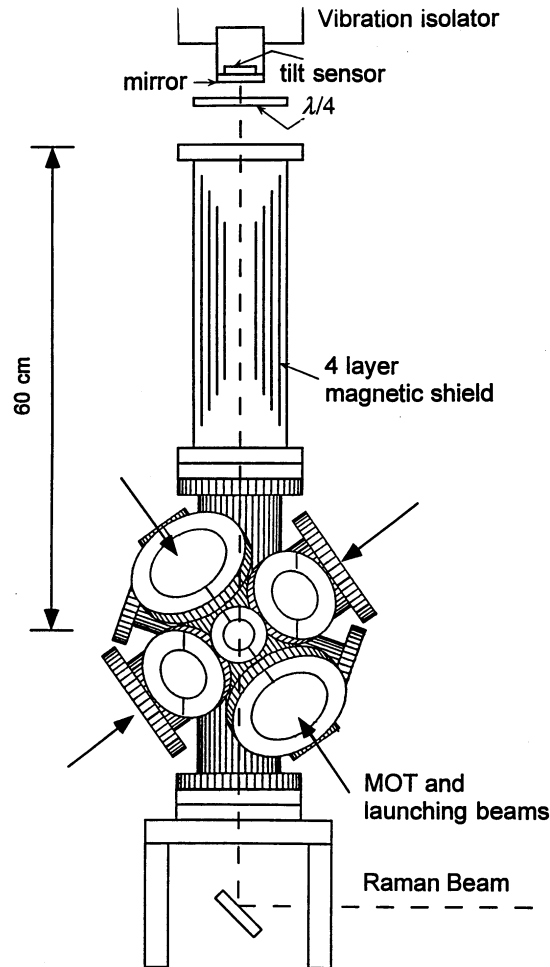
Figure 2. A schematic diagram of the vacuum chamber used in the measurement of g. The two Raman beams enter the can from below and are retro-reflected by a mirror mounted on a vibration isolation platform above the chamber. The chamber is mounted on a standard vibration isolation laser table stabilized with respect to the vertical direction by using a tilt sensor mounted on the back of the retro-mirror as part of a feedback system.

isolated platform is used to correct the vibrationally induced frequency jitter of the two independent, counterpropagating laser beams.

4. Experimental results

The experimental sequence is summarized as follows. Caesium atoms are captured in a magneto-optical trap in a low density vapour cell shown in figure 2. After *ca.* 0.6 s, the atoms are further cooled in polarization gradient molasses by shifting the frequencies of the molasses beams from a detuning of 20 to 60 MHz, and then launched upwards by shifting the relative frequencies of the molasses beams. In the final stages of the launch, the light intensity is ramped down in 300 μs so that the atoms can be adiabatically cooled to still colder temperatures (1.3–1.5 μK). Since our experiment is not shot noise limited, atoms in the $|F = 3, m_F = 0\rangle$ state within
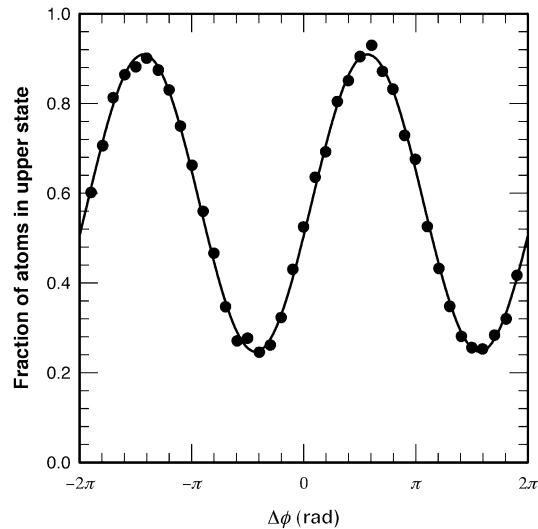
Figure 3. An example of typical interferometer fringes taken with $2T = 0.32$ s measurement time. Each data point corresponds to a single launch of the atoms. The total frequency shift during the interferometer drift time is 7.4 MHz and the linewidth of these fringes is 6 Hz. After a minute of integration time, the phase shift is determined with an uncertainty $\Delta g/g \cong 3 \times 10^{-9} \cong 0.01$ rad.

a narrow slice of the initial velocity distribution are selected through a series of stimulated microwave and optical pulses in order to increase the interferometer contrast. Stimulated Raman pulses generated by two phase-locked diode lasers are used to produce the interferometer pulses when the atoms are inside a quadruple magnetic shielded region with a bias field of 2 mG. The population of atoms in the $|4, 0\rangle$ state is measured for each launch by recording the fluorescence from the atoms illuminated by circularly polarized light tuned to $F = 4$ ground state to $F' = 5$ excited state transition. Next, the remaining atoms in the $F = 3$ state are transferred to the $F = 4$ state and the fluorescence measurement is repeated in order to measure the total number of atoms that have made it to the detection region.

Figure 3 shows the interferometer fringes for an interferometer time $2T$ of 0.32 s. Each data point represents a single launch of atoms. We emphasize the equivalent of 7.4×10^6 cycles of phase have accumulated during the measurement time. The short term stability of the interferometer is $\Delta g/g \cong 3 \times 10^{-9}$ after one minute of data taking. Figure $4a$ shows the results of over two days of continuous data taken with our atom interferometer. The data are plotted with a tidal model that includes only the elastic deformation of the earth and another model that also adds ocean loading effects. Figure $3b$ shows the difference between the data and the two tidal models. Each data point corresponds to an integration time of one minute. The statistical uncertainty for this data is $\Delta g/g \leqslant 1 \times 10^{10}$.

The absolute measurement in g of our atom interferometer was also compared to a falling corner cube instrument† which has an estimated absolute accuracy of about two parts in 10^9. After accounting for the difference in the heights of the two instruments, our preliminary value of g differs from the falling corner cube instrument by 140 parts per billion (the discrepency is less than 10 ppb as of September 25, 1997).

† The instrument is an FG5 interferometer manufactured by Micro-g and run by NOAA, the National Oceanic and Atmospheric Agency.
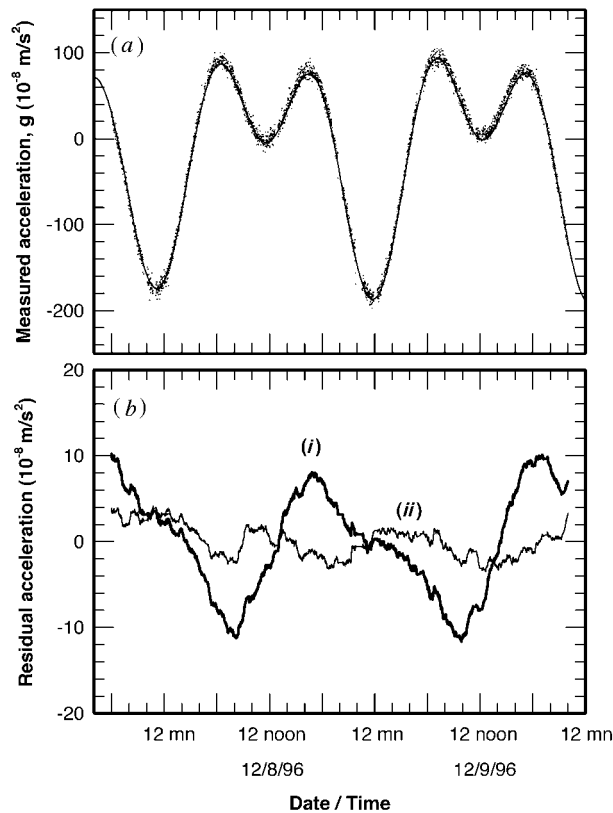
Figure 4. (*a*) An example of a continuous measurement of *g* for over two days. Each data point corresponds to a one minute averaging time. The solid curve is a model of Earth tides at Stanford, CA, on the days when the data were taken. (*b*) The residuals of the data with respect to a tidal models where (i) the Earth is modelled as a solid elastic object and where (ii) the effects of ocean loading of the Earth are taken into account. Effects at the few parts per billion level, like the phase shifts due to the time delays of the local tides or the effects of changing local barometric pressure, have not been included.

(A vertical distance of 1 m corresponds to a change in *g* of three parts in 10^7.) This discrepancy is to be compared to the neutron interferometer value of *g* which differs from a macroscopic measurement of *g* by a few percent in a series of measurements taken over the last 20 years (for a recent review, see Werner 1996).

We are in the process of identifying and correcting systematic effects. A detailed discussion of these effects will be given in a future publication. We are hopeful that systematic effects of this instrument can be understood at the level of one part per billion level or less. Also, the frequency of the D_2 line has an uncertainty of 40 ppb and is currently being measured with much higher accuracy by T. W. Hänsch and co-workers.

5. A measurement of $\hbar/M$

When an atom at rest absorbs a photon, conservation of momentum and energy demand that the energy of the photon $\hbar\omega_L$ must be slightly greater than the energy

level splitting $\hbar\omega_0$ of the atom. This frequency difference is given by

$$\frac{\omega_{\mathrm{L}} - \omega_0}{\omega_{\mathrm{L}}} = \frac{\hbar\omega_{\mathrm{L}}}{2Mc^2}. \tag{5.1}$$

Thus, the quantity $\hbar/M$ can be measured in terms of frequencies and a frequency shift. The fine structure constant α can be written as

$$\alpha = \left(\frac{2R_\infty}{c}\right)\left(\frac{M_{\mathrm{Cs}}}{m_{\mathrm{e}}}\right)\left(\frac{h}{M_{\mathrm{Cs}}}\right). \tag{5.2}$$

Since the Rydberg constant R_∞ and the mass ratios $M_{\mathrm{Cs}}/m_{\mathrm{p}}$ and $m_{\mathrm{p}}/m_{\mathrm{e}}$ can be determined with accuracy of the order of a few parts per billion, a measurement of the photon recoil frequency of comparable accuracy will yield a better value of α.

At present, α is determined by a range of measurements in elementary particle physics, atomic, and condensed matter mesoscopic and macroscopic systems. Comparison of various accurate measurements of α constitute one of the most demanding tests of the consistency of physics (for a review, see Kinoshita 1996). The most accurate determination of α is found by equating the quantum electrodynamic calculation of the magnetic moment of the electron with the measured value. Assuming that both the experiment and theory are correct, a value of α can be deduced with an uncertainty of 4.2 ppb. Other accurate measurements of α include measurements based on the muonium hyperfine structure, the quantum Hall effect, neutron diffraction and the AC Josephson effect with relative uncertainties of 134, 24, 39 and 56 ppb, respectively.

The first measurement of the recoil frequency shift was made in an heroic experiment by Hall *et al.* (1976). They achieved a resolution $\Delta\nu/\nu = 2.3 \times 10^{-3}$ using a laser stabilized to 200 Hz linewidth, 32 cm diameter optics and an absorption cell with a 13 m path length. Systematic effects were responsible for a 6×10^{-3} discrepancy between the known value of $\hbar/M$ and the recoil value. Our goal is to improve this measurement by another six orders of magnitude with an atom interferometric measurement. Currently, we have a precision in α of 10 ppb after two hours of integration time and are checking for possible systematic effects. Ultimately, we are hopeful that we can measure α with an absolute accuracy that rivals the $g-2$ determination of α.

Our approach to this measurement has been described elsewhere (Weiss *et al.* 1993, 1994; Weitz *et al.* 1994*a*,*b*; Young 1997). The improvement to the sensitivity and accuracy of our measurement is due to several factors. (i) We use transitions between magnetically insensitive ground states of the atom in a Ramsey–Bordé interferometer with a $\frac{1}{2}\pi - \frac{1}{2}\pi - \frac{1}{2}\pi - \frac{1}{2}\pi$ pulse sequence shown in figure 5. The interferometer uses an atomic fountain of laser cooled atoms with a measurement time corresponding to a linewidth of 8 Hz. (ii) As in our measurement of g, the counterpropagating beam geometry converts an ultra-high resolution optical spectroscopic experiment into an essentially microwave measurement. (iii) Our experiment measures the frequency shift of two interferometers and benefits from the cancellation of many systematic effects that are common to both interferometers. (iv) We have used an adiabatic method of transferring momenta to the atoms based on independently *tailoring the shape* of the two counterpropagating optical pulses. This method achieves a coherent Doppler sensitive efficiency of *ca.* 92%. (v) The high transfer efficiency enables us to increase the sensitivity of the measurement by adding many additional π pulses in between the two pairs of $\frac{1}{2}\pi$ pulses (see figure 5). With the insertion of 40 π pulses, the two sets of Ramsey fringes are separated by $(160 + 4)$ single photon recoils.
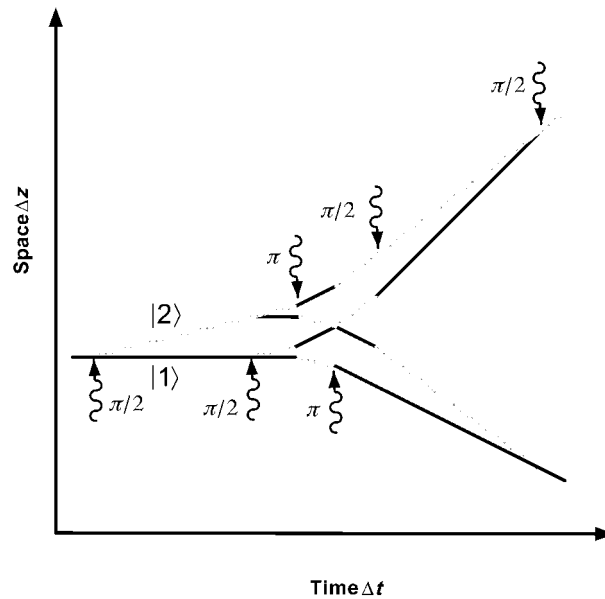
Figure 5. A spacetime diagram of the interferometer used to measure $\hbar/M_{Cs}$. The arrows indicate the direction of the effective photon momenta in the adiabatic transitions. For the sake of clarity, the acceleration due to gravity has not been included in this diagram. The free-fall time for this interferometer is comparable to the g measurement. Typically 30–50 π pulses are inserted in between the two $\frac{1}{2}\pi - \frac{1}{2}\pi$ pulse sequences in order to increase the sensitivity of the recoil measurement.

There are a large number of experimental parameters that have to be checked in this experiment. Any variation in the value of $\hbar/M$ due to a change in the magnetic fields, the atomic trajectory, the number of π pulses used in the measurement, the intensity of the pulses, the tilt of the table, etc., implies a systematic error. We have already determined that a number of potential effects such as Zeeman shifts, AC Stark shifts, missed photon kicks, laser beam collimation and alignment and coriolis phase shifts are below the 1 ppb level (see Young 1997). Microwave phase shifts, a possible coupling of changing magnetic fields to the vibration isolation system and the effect of wavefront distortion are currently being examined.

In addition to the measurement of $\hbar/M$, various other auxiliary quantities are needed to determine α. The largest uncertainty (45 ppb) is the absolute determination of the frequency of the D_1 line of caesium. T. W. Hänsch and co-workers plan to determine the value of both the D_1 and D_2 lines of caesium to an accuracy of better than 0.1 ppb. The next largest uncertainty is the proton to caesium mass ratio (40 ppb). D. Pritchard and co-workers are in the process of improving this mass ratio by at least another order of magnitude. Eventually, the mass ratio measurements may be the limiting factor in determining α.

6. Future improvements to precision atom interferometry

The sensitivity of atom interferometers using laser cooled atoms can be further increased. A number of improvements that should increase the sensitivity of our current interferometers include: (i) optical table rotational stabilization to complement our current vertical stabilization; (ii) reduced amplitude noise in our optical pulses, particularly in the $\hbar/M$ measurement where we use a large number of π pulses;

(iii) cleaner digital frequency synthesis of the microwave signals; and (iv) improved π pulse efficiency for the $\hbar/M$ measurement.

In our next generation of experiments, we plan to use a sequence of N π pulses to increase the momentum separation between the two arms of the atom interferometers. If all other things are equal, this change will enhance the sensitivity of the g measurement by a factor N and of the $\hbar/M$ measurement by a factor of N^2. A measurement of $\hbar/M$ for a lighter mass atom such as Li, He or H may also give higher resolution, but the larger recoil effect has to be weighed against certain technical inconveniences. In addition, the improved source brightness of a large number of Bose condensed atoms would reduce many of the systematic effects looming at the 0.1 ppb level. Finally, our interferometers are based on single particle interference effects. A shot noise limited interferometer of this type has a sensitivity that scales as $N^{1/2}$, where N is the number of particles in the fountain. An interferometer based on N particle interference would have a sensitivity that scales as N would be highly desirable.

References

Berman, P. 1997 *Atom interferometry*. New York: Academic.

Feynman, R. P. & Hibbs, A. R. 1965 *Quantum mechanics and path integrals*. New York: McGraw-Hill.

Greenberger, D. M. & Overhauser, A. W. 1979 Coherence effects in neutron diffraction and gravity experiments. *Rev. Mod. Phys.* **51**, 43–75.

Hall, J. L., Bordé, C. J. & Uehara, K. 1976 Direct optical resolution of the recoil effect using saturated absorption spectroscopy. *Phys. Rev. Lett.* **37**, 1339–1342.

Hensley, J., Peters, A. & Chu, S. 1997 *Rev. Sci. Instrum.* (Submitted.)

Kasevich, M. & Chu, S. 1991 Atom interferometry using stimulated Raman transitions. *Phys. Rev. Lett.* **67**, 181–184.

Kasevich, M. & Chu, S. 1992 Measurement of the gravitational acceleration of an atom with a light-pulse atom interferometer. *Appl. Phys.* B **54**, 321–332.

Kinoshita, T. 1996 The fine structure constant. *Rep. Prog. Phys.* **59**, 1459–1492.

Storey, P. & Cohen-Tannoudji, C. 1994 The Feynman path integral approach to atomic interferometry. A tutorial. *J. Phys.* **4**, 1999–2027.

Weiss, D. S., Young, B. C. & Chu, S. 1993 A precision measurement of the photon recoil of an atom using atomic interferometry. *Phys. Rev. Lett.* **70**, 2706–2709.

Weiss, D. S., Young, B. C. & Chu, S. 1994 A precision measurement of $\hbar/M$ based on the photon recoil using laser cooled atoms and atom interferometry. *Appl. Phys.* B **59**, 217–256.

Weitz, M., Young, B. C. & Chu, S. 1994*a* Atom manipulation based on delayed laser pulses in three- and four-level systems: light shifts and transfer efficiencies. *Phys. Rev.* A **50**, 2438–2566.

Weitz, M., Young, B. C. & Chu, S. 1994*b* Atomic interferometer based on adiabatic population transfer. *Phys. Rev. Lett.* **73**, 2563–2566.

Werner, S. A. 1996 Quantum phase shifts induced by gravity and rotation. *J. Phys. Soc. Jap.* **65**, 51–61.

Young, B. C. 1997 Ph.D. thesis, Stanford University, CA.